Ferromagnetic properties of the degenerate semiconductor $Pb_{0.20}Sn_{0.72}Mn_{0.08}Te$

R. R. Gałązka
Institute of Physics, Polish Academy of Sciences, Al. Lotników 32/46, PL-02-668 Warszawa, Poland

J. Spałek,* A. Lewicki,† and B. C. Crooker
Department of Physics, Purdue University, West Lafayette, Indiana 47907

G. Karczewski and T. Story
Institute of Physics, Polish Academy of Sciences, Al. Lotników 32/46, PL-02-668 Warszawa, Poland
(Received 24 August 1990)

We analyze the properties of a diluted ferromagnetic semiconductor $Pb_xSn_{1-x-y}Mn_yTe$ for $x=0.20$ and $y=0.08$, for the two concentrations of holes $p=2.3\times10^{21}$ cm^{-3} and $p=2.7\times10^{20}$ cm^{-3}. We determine from the field dependence of the magnetization the magnon contribution to the spontaneous magnetization; this contribution is used to calculate the magnitude of the effective exchange integral $J_1=4.8$ K between nearest neighbors for the sample with higher p. The paramagnetic Curie temperature determined theoretically from the magnon contribution to the magnetization agrees within 30% with that obtained from measurements in the paramagnetic regime for the sample with higher p. The magnon contribution to the specific heat is estimated and subtracted from the corresponding data. The large value of the linear specific-heat coefficient $\gamma\approx73$ mJ/mol K^2, as well as the spin reduction $\Delta S\approx0.2\pm0.05$ of the atomic spin $S=\frac{5}{2}$ of the Mn^{2+} ion indicate an antiferromagnetic coupling of the Kondo type between the valence holes and the magnetic ions.

I. INTRODUCTION

In this paper we study the ferromagnetic properties of the diluted magnetic semiconductor $Pb_{0.0}Sn_{0.72}Mn_{0.08}Te$ and interpret these properties within the spin-wave theory for temperatures $T\ll T_c$, where T_c is the Curie temperature. The onset of ferromagnetism as a function of hole concentration has been reported earlier;[1] here we answer the question to what extent the magnetic state of this degenerate $A^{IV}B^{VI}$ mixed semiconductor can be regarded as a standard ferromagnet. The nontrivial character of this question becomes apparent if we represent the compound $Pb_{0.20}Sn_{0.72}Mn_{0.08}Te$ as a mixture $(PbTe)_{0.20}(SnTe)_{0.72}(MnTe)_{0.08}$, and hence recognize that for hole-carrier concentrations $p\geq10^{20}$ cm^{-3}, the long-range Ruderman-Kittle-Kasuya-Yosida (RKKY) interaction coexists with the superexchange Mn-Te-Mn interaction. The importance of the superexchange interaction in diluted magnetic (semimagnetic) $A^{II}B^{VI}$ semiconductors (DMS) with Mn has been discussed earlier.[2] This interaction is antiferromagnetic since the Mn^{2+} $3d$ shell is half filled and therefore, the admixture of the neighboring $5p$ (and $3d$) wave function $|j\sigma'\rangle$ to the $3d$ state $|i\sigma\rangle$ of a given Mn^{2+} ion is possible only for the spin state $\sigma'=-\sigma$. In the present narrow-gap semiconducting system, unlike the rare-earth metals, the carrier concentration can be changed[3] by more than an order of magnitude for fixed concentration x of magnetic ions and therefore, with growing p and low concentration, $x<0.1$, of Mn the system undergoes[4] an abrupt transition from a randomly diluted Heisenberg anti-ferromagnetic to a ferromagnetic semimetal. Such a transition has actually been observed recently[4] and for the $x=0.08$ samples studied here takes place at $p\approx2\times10^{20}$ cm^{-3}. The concentration x of magnetic ions is below the percolation threshold $x\approx0.17$ for short-range magnetic interaction; hence the exchange interaction in this system must be of long-range nature.

The structure of this paper is as follows. In the next section we summarize the experimental details. In Sec. III we determine the spin-wave contribution to the magnetization for the sample with hole concentration $p=2.3\times10^{21}$ cm^{-3}, as well as calculate the effective magnitude of the exchange integral J_1. The value $J_1\approx4.3$ K is used to estimate theoretically the paramagnetic Curie temperature $\Theta=(\frac{2}{3})J_1zS(S+1)\approx25$ K which roughly agrees with that determined experimentally $\Theta\approx18$ K. We also estimate the magnon contribution to the specific heat which is subtracted from the measured specific heat for this system. The results are presented in Sec. IV. The magnetic part of the specific heat exhibits a peak which can be attributed to the ferromagnetic phase transition with a critical temperature $T_c\approx12.3$ K. The low-temperature part of the specific heat is linear in T, with a very large value of the linear coefficient $\gamma\approx912$ mJ/K^2 mol Mn. Such a large value of γ, in conjunction with about a 10% diminution of the effective spin value from its atomic value $S=\frac{5}{2}$ is attributed to an antiferromagnetic coupling of the Kondo-type between the holes and the Mn^{2+} spins.

II. EXPERIMENTAL TECHNIQUES

Samples were prepared by the Bridgman technique. In order to change the carrier concentration, samples were

annealed in either Te- or Sn-rich atmospheres at $T \approx 700$°C. To determine the hole concentration, Hall voltage was measured at 77 K and in a magnetic field of $2T$. Electron microprobe analysis revealed good homogeneity of both Mn and Sn atom distributions in the samples. No second-phase inclusions were observed in x-ray measurements.

The magnetic susceptibility and the magnetization measurements were carried out using a vibrating-sample magnetometer operating at a frequency of 82 Hz. The system was calibrated with a sphere of high-purity nickel. The magnetic field was monitored using a multirange gaussmeter. The highest available resolution ΔH of this gaussmeter is equal to 0.01 Oe. The earth's magnetic field was not completely compensated. Therefore, statements "zero field" or "zero-field cooling (ZFC)" used in this article mean that, strictly speaking, the magnetic field is not larger than ≈ 0.2 Oe.

The sample temperature was varied between 2 and 295 K with a cryogenic temperature controller with a stability $\Delta T/T$ better than 0.01. A very small signal from the empty sample holder ($\approx 3\times 10^{-4}$ emu at 9 kOe) was subtracted from the susceptibility data for $T > T_c$. Below T_c, this correction is not significant, since it constitutes less than 0.1% of the total susceptibility.

The specific heat measurements were made in a conventional ^{3}He cryostat using the heat-pulse technique. The addenda heat capacity was subtracted from the data. This correction was less than 10% of the total heat capacity in the linear region of Fig. 10 (see below).

III. MAGNETIC MEASUREMENTS AND THEIR ANALYSIS

In this section we analyze the temperature and applied magnetic field dependences of the magnetization. In Figs. 1 and 2 we present a family of curves representing the field dependence of the magnetization $M = M(H)$ for different temperatures and for the sample with $p = 2.3\times 10^{21}$ cm^{-3}. The rapid growth of M is connected with the disappearance of the domain structure; the material is magnetically very soft and the coercive field is $H_c \approx 1$ Oe. The part of the magnetization curve for the applied field $H \gg H_c$ is fitted to the straight line $M(H,T) = M_0(T) + \chi_f H$, where the remanent part $M_0(T)$ obtained in this way is regarded as the spontaneous magnetization at temperature T, and χ_f is the zero-field susceptibility for a single domain sample. The quality of the fits in Figs. 1 and 2 is quite good for temperatures which are substantially lower than the Curie temperature $T_c \approx 12.3$ K.

The temperature dependence of the spontaneous magnetization obtained this way is displayed in Fig. 3. The $M_0(T)$ dependence when extrapolated to $T = 0$ supplies the value of the saturation magnetization $M_s = M_0(0) = 7.18$ emu/g. If we take the atomic spin $S = \frac{5}{2}$ for Mn^{2+} ions, then we obtain the saturation value for $M_s = N_{AV} g \mu_B S x / M_{av} = 8.63$ emu/g, where we have assumed that the concentration of manganese is $x = 0.08$, and the Landé factor $g = 2$; N_{AV} and μ_B are Avogadro's number and the Bohr magneton, respectively. The lower

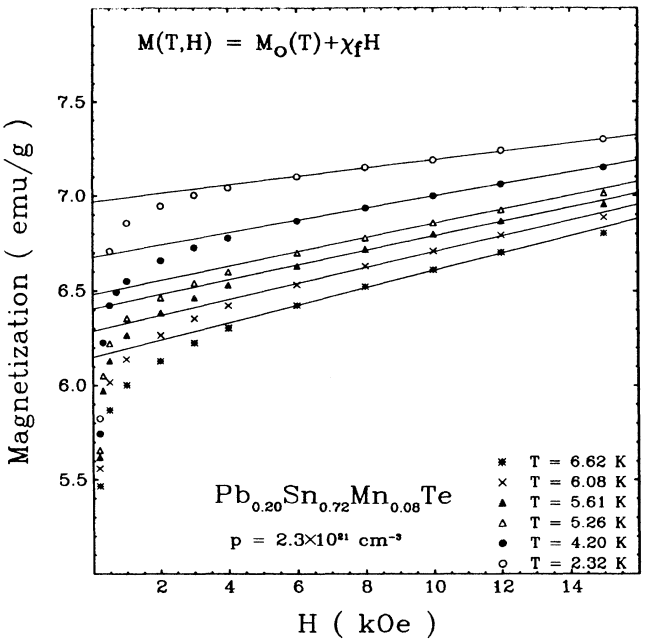

FIG. 1. Field dependence of the magnetization for the temperatures specified. The straight lines $M(H) = M_0(T) + \chi_f H$ are used to determine the spontaneous magnetization $M_0(T)$ in the single-domain configuration.

than atomic value obtained from the extrapolation to $T = 0$ in Fig. 3 can be accounted for if we take a smaller concentration x by about 20%; an alternative explanation involving reduction of the Mn^{2+} spin value to $S = 2.1$ due to a compensating character of the carriers will be presented below.

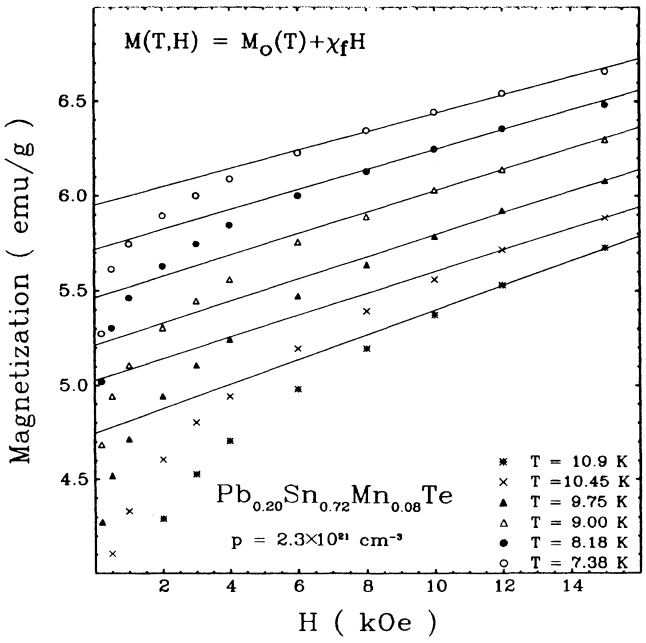

FIG. 2. Same as in Fig. 1 for higher temperatures.

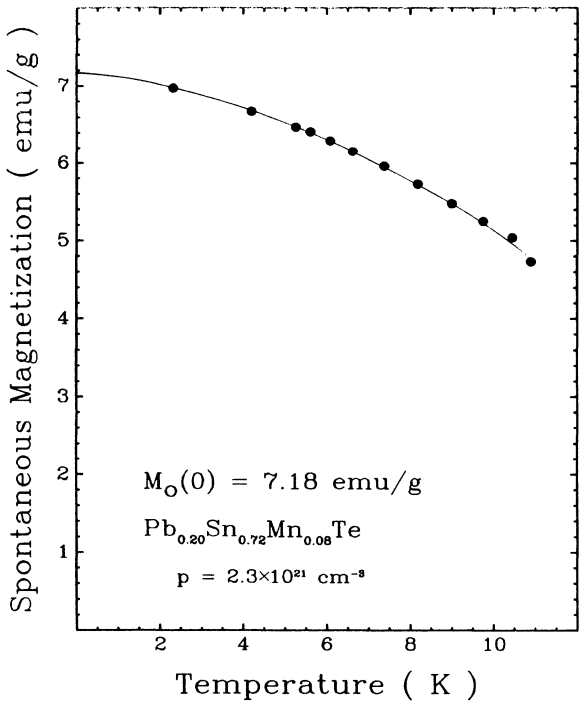

FIG. 3. Temperature dependence of the spontaneous magnetization. The saturation magnetization $M_s = 7.18$ emu/g has been obtained by extrapolating the data to $T = 0$. The solid line is provided as a guide to the eye.

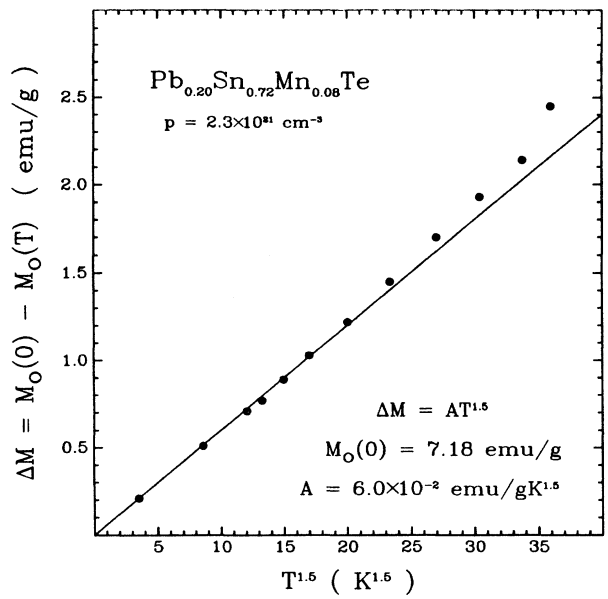

FIG. 4. Deviation of the magnetization $M_0(T)$ from the saturation value vs $T^{3/2}$. The straight line is the least-squares fit to the data, with the coefficient of proportionality $A = 0.06$ emu/g $K^{3/2}$.

In order to verify that the magnetization reduction with increasing T is caused by thermal excitations of magnons we have plotted in Fig. 4 the difference $\Delta M \equiv M_S - M_0(T)$ vs $T^{3/2}$. A well-defined linear dependence is observed in the lower-temperature range, as expected from the spin-wave theory.[5] The constant of proportionality is $A = 0.060$ emu/g $K^{3/2}$, or equivalently, 15.7 emu/mol $K^{3/2}$. Taking the lattice constant of PbSnTe as $a \approx 6.32$ Å we can determine the magnitude of the effective exchange integral J_1 from the relation $A = 0.117(\mu_b/s^3)k_B^{3/2}/(2J_1S)^{3/2}$ for the fcc structure, where k_B is the Boltzmann constant, and S is the spin magnitude. Taking $S = \frac{5}{2}$ we have that $J_1 \approx 4.8$ K, and the value of the exchange stiffness constant $D = 2J_1Sa^2 \approx 9.6 \times 10^{-14}$ K Å^2. Note that J_1 expresses the effective interaction between nearest neighbors. Such representation is feasible in our system with a long-range (RKKY) interaction since the microscopic parameters determined here depend only on the total strength of the exchange interaction $-\sum_{j(i)} J_{ij}$. The effective integral $J_1 \equiv (1/z)\sum_{j(i)} J_{ij}$ serves as an input parameter to evaluate the paramagnetic Curie-Weiss temperature $\Theta = (\frac{2}{3})J_1 z x S(S+1)/k_B \approx 25$ K, where $z \equiv 12$ is the number of nearest cation neighbors.

To determine the Curie temperature we have measured the temperature dependence of the magnetic moment in the interval from 4.2 K to 300 K. In Fig. 5 we display the magnetic moment in the applied field $H = 3$ Oe, measured either in a cooling cycle or in a heating cycle following zero-field cooling. The two measurements do not provide the same results below the transition (Curie) temperature $T_c = 12.3$ K; the difference in magnetic moment in these two situations is attributed to the presence of a domain structure below T_c if the sample is cooled in zero field (note that the field $H = 3$ Oe applied during the mea-

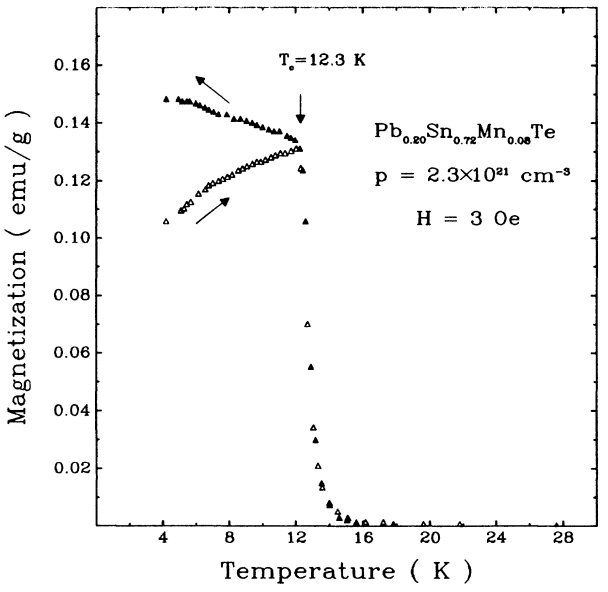

FIG. 5. Temperature dependence of the magnetization for the sample with hole concentration $p = 2.3 \times 10^{21}$ cm^{-3}. The open triangles are obtained on heating cycle after cooling in zero applied magnetic field. The full triangles correspond to measurement of the magnetic moment on cooling in the field $H = 3$ Oe. The Curie point $T_c = 12.3$ K is denoted by the arrow.

surements is comparable to the coercive field and much smaller than the field saturating the magnetization at a given T).

The method of T_c determination shown in Fig. 5 is accurate only in the case when the concentration of holes is high enough to make the ferromagnetic part of the RKKY interaction dominant in the whole sample. In Fig. 6 we show $M(T)$ curves for the sample with hole concentration $p=2.7\times10^{20}$ cm^{-3}. The difference between the curve measured while cooling in the field $H=3$ Oe, and that obtained in the heating cycle following cooling in the absence of the field is less sharply defined in this case. Because of the lack of a sharp distinction between the para- and ferromagnetic regimes for this sample we perform the detailed analysis of the results only for the system with $p=2.3\times10^{21}$ cm^{-3}. Note also that the difference between the curves in Fig. 6 cannot be ascribed to a spin-glass behavior since the magnetic moment grows spectacularly near T_c and the large value of the moment levels off upon further decrease of temperature. At best, the sample with $p=2.7\times10^{20}$ cm^{-3} may be regarded as magnetically inhomogeneous.

In connection with the determination of T_c presented in Figs. 5 and 6 one should say that the method is suitable for magnetically soft materials such as the compounds studied here. For such materials the classical method of determining T_c from the maximum of the derivative dM/dT in a given field H is less accurate. For an explicit illustration we have plotted in Fig. 7 the $M(T)$ dependence for the sample with $p=2.3\times10^{21}$ cm^{-3} in the two fields, 100 Oe and 10 kOe. The value of T_c determined from Fig. 5 has also been marked. The field $H=100$ Oe already smears out the singular behavior of

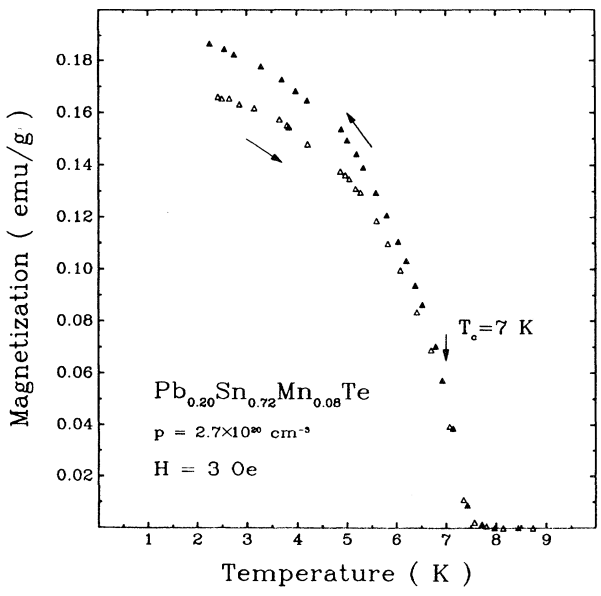

FIG. 6. Same as in Fig. 5 for the sample with $p=2.7\times10^{20}$ cm^{-3}. The continuous line is a guide to the eye; it marks an approximate position of the point of coalescence ($T_c\approx7$ K) of the two curves.

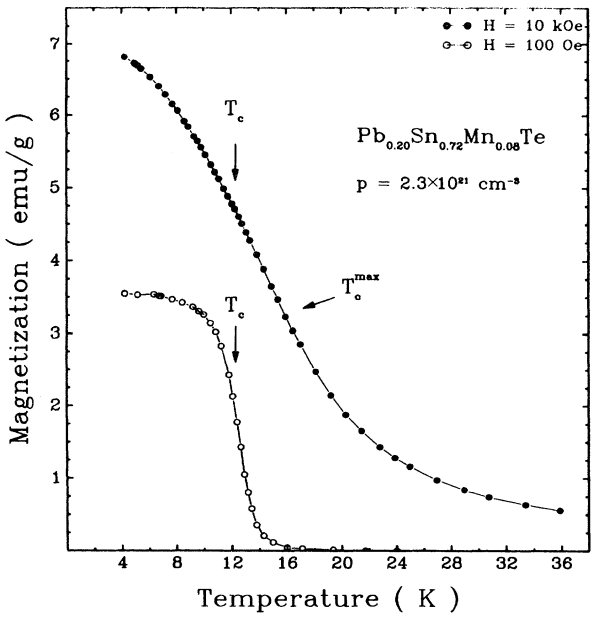

FIG. 7. Temperature dependence of the magnetization in applied fields $H=100$ Oe and 10 kOe, respectively. Note that the value of T_c determined from the maximum slope of dM/dT does not coincide with that determined in Fig. 5. The continuous lines are guides to the eye.

dM/dT at T_c. Additionally, the position $T_c^{\max}$ of the inflection point on the $M(T)$ curve does not coincide with the value of T_c determined in the much smaller field of Fig. 5. Also, $T_c^{\max}$ depends on the magnetic field. Because of these reasons we conclude that our method of determining T_c in Fig. 5 is more reliable and accurate. To the best of our knowledge, this method has not been used before to determine T_c in a multidomain sample.

The value of $T_c\approx7$ K determined in Fig. 6 for the sample with $p=2.7\times10^{20}$ cm^{-3} exceeds the value $\Theta\approx4$ K obtained from the Curie-Weiss law. We attribute this inconsistency to the inhomogeneity of samples with carrier concentration close to the threshold of disappearance of ferromagnetism.[4] The physical origin of this discrepancy is not understood at this time.

The sign of the effective exchange integral is determined directly from the Curie-Weiss law for the magnetic susceptibility shown in Fig. 8 for the sample with $p=2.3\times10^{21}$ cm^{-3}. The data are fitted to the formula $\chi=C_0x/(T-\Theta)$, with $C_0=3.84$ cm^3 K/mol Mn, and $\Theta=19$ K. The Curie constant $C_0\equiv(g\mu_B)^2S(S+1)N_{\rm AV}/3k_B$ provides the effective Mn^{2+} spin value $S=2.31\pm0.05$, whereas the Curie-Weiss temperature

$$\Theta=2x\sum_{j(i)}J_{ij}S(S+1)/3$$

$$\equiv2J_1zxS(S+1)/3$$

provides the effective exchange integral $J_1\approx4$ K. As in the case of $M_0(0)$ determined before, the spin value is again lower than the pure atomic value $\frac{5}{2}$; the J_1 value

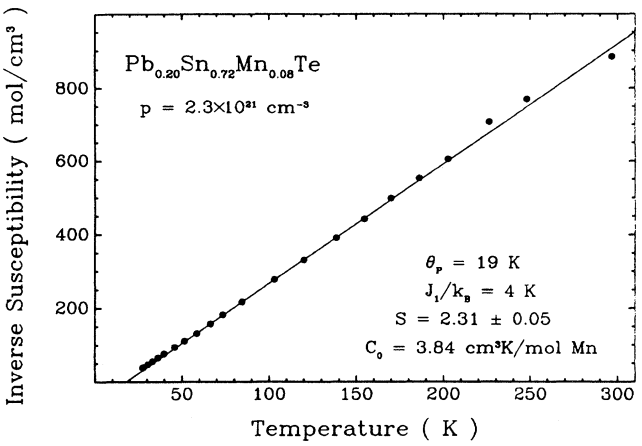

FIG. 8. Temperature dependence of the inverse magnetic susceptibility for the sample with hole concentration $p=2.3\times10^{21}$ cm^{-3}. The straight line represents the Curie-Weiss law fit with the Curie constant $C_0=3.84$ cm^3 K/mol Mn, and the paramagnetic Curie temperature $\Theta_0=19$ K.

agrees within 30% with that estimated before from the spin-wave correction to the static magnetization. Also, the measured value of Θ is about 50% higher than the T_c value, a typical feature of ferromagnetic systems with localized magnetic moments.

To demonstrate the influence of carrier concentration on both the magnitude of the spin and the strength of the exchange interaction we display in Fig. 9 the temperature dependence of the paramagnetic susceptibility for the same Mn concentration $x=0.08$, but for the carrier concentration $p=2.7\times10^{20}$ cm^{-3}. The corresponding values extracted from the Curie-Weiss law fit to the data are $S=2.4\pm0.1$ and $J_1=0.8$ K. The value of spin is higher and the strength of the ferromagnetic interaction decreased by a factor of 5 compared to the sample with

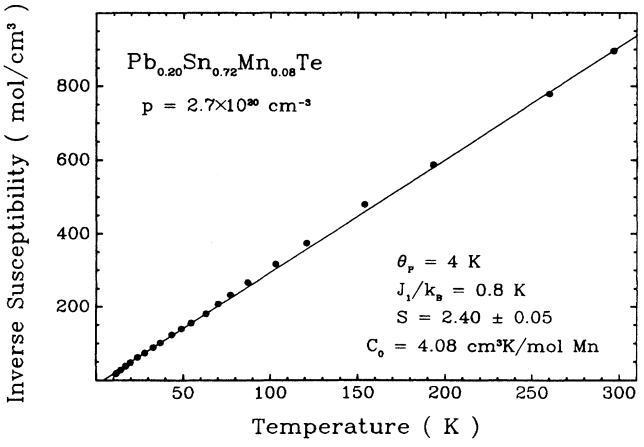

FIG. 9. Same as in Fig. 8 for the sample with $p=2.7\times10^{20}$ cm^{-3}.

$p=2.3\times10^{21}$ cm^{-3}. On the basis of this comparison we strengthen the conclusion reached before[1,3,4] that the RKKY interaction is responsible for the ferromagnetic ordering. Also, the diminution of the atomic spin, smaller for the lower p, can be ascribed to an antiferromagnetic coupling of the Kondo type between the holes and the Mn^{2+} spins. This conjecture will be discussed further in the next section, where we analyze the specific heat data.

Summarizing, we have shown in this section that the compound $Pb_{0.2}Sn_{0.72}Mn_{0.08}Te$ can be regarded as a Heisenberg ferromagnet with reduced spin of the Mn^{2+} ion. Both the paramagnetic (Curie-Weiss) and critical (Curie) temperatures depend strongly on the carrier concentration. The carrier induced (RKKY) interaction is stronger than the superexchange interaction; otherwise, one would have a negative sign of the Curie-Weiss temperature[2] and the absence of any magnetic ordering (including spin-glass behavior) above 1 K for such a low concentration of magnetic ions.

IV. LINEAR SPECIFIC HEAT AND ITS INTERPRETATION

In the foregoing section we have determined the exchange stiffness constant $D=9.6\times10^{-14}$ K Å^2, with the help of which one can determine the magnon contribution to the specific heat C. For $T\rightarrow0$ it is equal to[5]

$$C=2[0.113R\,(k_BT/D)^{3/2}]\ ,$$

where R is the gas constant. Explicitly,

$$C=1.18T^{3/2}\ \text{mJ/K mol}\ .$$

We have determined the temperature dependence of the specific heat and the detailed data will be presented elsewhere.[6] In Fig. 10 we present $C(T)$ data for the sample with $p=2.3\times10^{21}$ cm^{-3} from which the lattice part has been subtracted. The Debye temperature $\Theta_D=135$ K has been determined from $C(T)>T_c$ and for the sample with $T_c\approx7$ K. Three specific features of these data should be noted. First, the data have a wide maximum in the region of $T_c\approx11\pm1.5$ K encompassing the critical point determined above from the $M(T)$ behavior. Unfortunately, a scattering of the data points does not allow us to draw any detailed conclusions about character of the critical behavior near T_c. Second, the specific heat is reduced in the magnetic field $H=1$ T, an effect expected since both magnon and critical fluctuations are reduced in the applied magnetic field. Third, a clear linear dependence of $C(T)$ at lower temperatures $T\leq8$ K for this sample is detected.

To study this linear behavior in detail we have subtracted the magnon contribution from the $H=0$ data. This procedure did not essentially alter the observed $C\sim T$ behavior. In general, the magnon contribution is small for $T\geq4$ K; for example, for $T=5$ K the magnon contribution is ≈13 mJ/K mol, whereas the experimental value is much higher (250 mJ/K mol). The linear behavior must then be attributed to an electronic contribution since the two-level lattice contribution to the linear specific heat in the disordered systems is much smaller.[7]

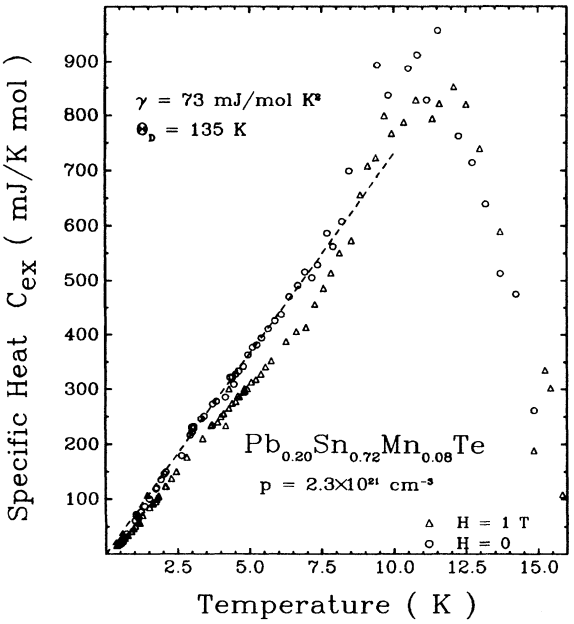

FIG. 10. The specific heat as a function of temperature, with the lattice contribution ($\sim T^3$) and magnon ($\sim T^{3/2}$) contribution subtracted. The straight line represents the linear part of the specific heat $C=\gamma T$, with $\gamma \approx 73$ mJ/mol K^2. The open circles represent the $H=0$ data, whereas the solid circles those in the field $H=10$ kOe.

If we represent the low-T data in the form $C=\gamma T$, then $\gamma \approx 73$ mJ/mol K^2 is very large. Such a large electronic contribution must be connected with the presence of Mn ions since the system $Pb_{1-x}Sn_xTe$ represents a rather standard degenerate semiconductor or semimetal. In such a situation the value of γ calculated per mol of Mn is even much larger and equal to $\gamma/x \approx 912$ mJ/K^2 mol Mn. The enormous value of γ is observed only in one kind of systems, namely, in the Kondo-lattice (heavy fermion) and impurity-Kondo systems.[8] It is tempting to interpret this type of behavior as due to heavy holes which are indeed coupled antiferromagnetically to the Mn^{2+} spins.[9] However, a confirmation of this hypothesis, which also explains naturally the Mn^{2+} spin reduction[10] discussed above, requires a detailed study of the temperature dependence of the resistivity and of the negative magnetoresistance in higher fields. Such measurements may not be easy to interpret because of the effect of cation alloying on the scattering of carriers; nonetheless, they are certainly worth pursuing since these systems provide a unique opportunity to study the effects of variable carrier concentration on the Kondo-singlet or Kondo-lattice formation. The sample with lower $p=2.7\times10^{20}$ cm^{-3} did not show such clear linear T behavior of the specific heat. In that system the carrier concentration is lower than that of the magnetic ions; hence the Kondo-type correlations will be largely reduced.

Very recently, the effective mass of the heavy holes has been estimated[11] from the combined analysis of the reflectivity spectrum, low-field Hall effect, and the electrical conductivity. It has been found that the effective mass of heavy holes is $m^*=(1.7\pm0.2)\,m_0$, where m_0 is the free electron mass. Taking $m^*\approx 2m_0$ and counting all 12 band minima along the Σ direction (with heavy holes) we obtain the heavy-hole contribution to the linear specific heat coefficient $\gamma \approx 24\gamma_0$, where γ_0 is the coefficient for the electron gas of the same density. This already large value of γ is still by a factor of 3 too small to account fully for the observed value $\gamma \approx 73$ mJ/mol K^2. However, the m^* value quoted above was determined at 77 K; an essential increase by a factor 2–3 could take place with decreasing temperature.

A large linear specific heat ($C\sim T$) has been observed in both metallic spin-glass systems *Cu*Mn and *Au*Fe,[12,13] and in the $Cd_{1-x}Mn_xTe$ semimagnetic semiconductor.[14] We do not think that such an interpretation of the low-T part of the specific heat applies to the results presented in Fig. 10. This is because the dominant exchange interaction is ferromagnetic and the remanent magnetization does not change appreciably with time in the low-temperature regime $T<T_c$. Also, a mixture of spin-glass and ferromagnetic phases cannot be regarded as a realistic representation of the magnetic state because of the same reasons.

V. CONCLUSIONS

In this paper we have analyzed the magnetic and thermal properties of the randomly diluted Mn^{2+} spin subsystem in the narrow-gap degenerate semiconductor $Pb_{0.20}Sn_{0.72}Mn_{0.08}Te$. We believe that we have proved that the material is a ferromagnet. This is because (i) the paramagnetic Curie-Weiss temperature is positive; (ii) the low-temperature part of the magnetization decreases with T in accordance with the spin-wave theory prediction; and (iii) the susceptibility grows spectacularly when the critical temperature T_c is approached. Furthermore, the material is magnetically very soft since the Mn^{2+} ions are in the singlet orbital momentum state, and therefore the spin-orbit interaction contribution to the magnetocrystalline anisotropy is absent. Additionally, due to the half-filled $3d$ shell of the Mn^{2+} ion, spin subsystem is coupled antiferromagnetically to the valence holes; this coupling is suggested to produce a diminution of the Mn^{2+} spin of the order 10–15 % via the Kondo effect. In this respect the present material may prove unique for studies of a coexistence of the Kondo behavior and a ferromagnetic ordering. The Kondo coupling may also explain the dramatic effects observed on the carrier states, namely, it can lead to the large value of the linear specific heat coefficient γ. If our interpretation of the observed linear specific heat is correct, then the hole quasiparticles should have strongly renormalized properties such as the effective mass or the g-factor. It should be possible to detect this effect in de Haas-van Alphen or related quantum transport measurements in a magnetic field. The interesting feature of the system studied is the possibility of changing the carrier concentration in a wide range ($p\sim10^{20}$ cm^{-3}). The Kondo-type of effect should appear significant for $p\gg x$. In this regime the Kondo and RKKY interactions may produce both ferromagnetic ordering and a strong renormalization of the carrier states. For example, the spin splitting of the carrier states

should differ from that calculated in the mean-field approximation, i.e., it should not scale linearly into $M_0(T)$.

ACKNOWLEDGMENTS

The authors are grateful to Professor Pieter Keesom for his help and advice during the specific-heat measurements. One of the authors (J.S.) acknowledges the support of the Superconductivity Research Center at Purdue University. A.L. was supported by the Materials Research Group Grant No. DMR-89-13706. Magnetic measurements were performed using the instrumentation of the Indiana Center for Innovative Superconducting Technology.

---

*Current address: Institute of Theoretical Physics, Warsaw University, ul. Hoża 69, PL-00-681 Warszawa, Poland.

†On leave from Department of Solid State Physics, AGH Technical University, PL-30-059 Kraków, Poland.

[1]T. Story, R. R. Gałązka, R.B. Frankel, and P. A. Wolff, Phys. Rev. Lett. **56**, 777 (1986); H. J. M. Swagten, W. J. M. de Jonge, R. R. Gałązka, P. Warmenbol, and J. T. Devreese, Phys. Rev. B **37**, 9907 (1988).

[2]J. Spałek, A. Lewicki, Z. Tarnawski, J. K. Furdyna, R. R. Gałązka and Z. Obuszko, Phys. Rev. B **33**, 3407 (1986); A. Lewicki, J. Spałek, J. K. Furdyna, and R. R. Gałązka, *ibid.* **37**, 1860 (1988).

[3]T. Suski, J. Igalson, and T. Story, J. Magn. Magn. Mater. **66**, 325 (1987).

[4]G. Karczewski, A. Wiśniewski, T. Story, and R. R. Gałązka, in *Proceedings of the 19th International Conference on Physics of Semiconductors, Warsaw, 1988,* edited by W. Zawadzki (Institute of Physics, Warsaw, 1988), pp. 1555–1558.

[5]See, e.g., C. Kittle, *Quantum Theory of Solids* (Wiley, New York, 1987), Chap. 4.

[6]R. R. Gałązka *et al.* (unpublished).

[7]P. W. Anderson, B. I. Halperin, and C. M. Varma, Philos. Mag. **25**, 1 (1972); W. A. Philips, J. Low. Temp. Phys. **7**, 351 (1972).

[8]See, e.g., Y. Ōnuki and T. Komatsubara, J. Magn. Magn. Mater. **63&64**, 281 (1987).

[9]The antiferromagnetic nature of this interaction is caused by $5p$-$3d$ hybridization since the $3d$ level is positioned within the $5p$ band limits, cf. A. K. Bhattacharjee, G. Fishman, and B. Cogblin, Physica B+C **117&118**, 449 (1983).

[10]A simple mean-field analysis of the system of carriers coupled to the Mn localized moments by the antoferromagnetic Kondo interaction leads to the reduction of the Curie constant by the factor $(1-|J|\rho)^2$, where J is the exchange integral and ρ is the density of states at the Fermi level; cf. Eq. (12) in J. Spałek and A. M. Oleś, Solid State Commun. **37**, 571 (1981). One should notice that this factor is larger for the higher concentration P, i.e., when the Fermi energy is placed in the Σ band due the heavy holes since $\rho \sim m^*$, where m^* is the effective mass of the holes.

[11]G. Karczewski, L. Swierkowski, T. Story, A. Szczerbakow, J. Niewodniczańska-Blinowska, and G. Bauer, Semicond. Sci. Technol. **5** (1990).

[12]L. E. Wenger and P. H. Keesom, Phys. Rev. B **13**, 4053 (1976).

[13]B. Dreyfus, J. Souletie, R. Tournier, and L. Weil, C. R. Acad. Sci. **259**, 4266 (1964).

[14]R. R. Gałązka, S. Nagata, and P. H. Keesom, Phys. Rev. B **22**, 3344 (1980).